

ARTICLE OPEN



The relationship between synaptic density marker SV2A, glutamate and *N*-acetyl aspartate levels in healthy volunteers and schizophrenia: a multimodal PET and magnetic resonance spectroscopy brain imaging study

Ellis Chika Onwordi ^{1,2,3,4}✉, Thomas Whitehurst ^{1,2}, Ayla Mansur^{5,6}, Ben Statton ¹, Alaine Berry¹, Marina Quinlan¹, Declan P. O'Regan ¹, Maria Rogdaki ^{1,2,3,4}, Tiago Reis Marques ^{1,3,4}, Eugenii A. Rabiner ^{6,7}, Roger N. Gunn^{5,6}, Anthony C. Vernon ^{8,9}, Sridhar Natesan ^{1,3} and Oliver D. Howes ^{1,2,3,4}✉

© The Author(s) 2021

Glutamatergic excitotoxicity is hypothesised to underlie synaptic loss in schizophrenia pathogenesis, but it is unknown whether synaptic markers are related to glutamatergic function in vivo. Additionally, it has been proposed that *N*-acetyl aspartate (NAA) levels reflect neuronal integrity. Here, we investigated whether synaptic vesicle glycoprotein 2 A (SV2A) levels are related to glutamatergic markers and NAA in healthy volunteers (HV) and schizophrenia patients (SCZ). Forty volunteers (SCZ $n = 18$, HV $n = 22$) underwent [¹¹C]UCB-J positron emission tomography and proton magnetic resonance spectroscopy (¹H-MRS) imaging in the left hippocampus and anterior cingulate cortex (ACC) to index [¹¹C]UCB-J distribution volume ratio (DVR), and creatine-scaled glutamate (Glu/Cr), glutamate and glutamine (Glx/Cr) and NAA (NAA/Cr). In healthy volunteers, but not patients, [¹¹C]UCB-J DVR was significantly positively correlated with Glu/Cr, in both the hippocampus and ACC. Furthermore, in healthy volunteers, but not patients, [¹¹C]UCB-J DVR was significantly positively correlated with Glx/Cr, in both the hippocampus and ACC. There were no significant relationships between [¹¹C]UCB-J DVR and NAA/Cr in the hippocampus or ACC in healthy volunteers or patients. Therefore, an appreciable proportion of the brain ¹H-MRS glutamatergic signal is related to synaptic density in healthy volunteers. This relationship is not seen in schizophrenia, which, taken with lower synaptic marker levels, is consistent with lower levels of glutamatergic terminals and/or a lower proportion of glutamatergic relative to GABAergic terminals in the ACC in schizophrenia.

Translational Psychiatry (2021)11:393; <https://doi.org/10.1038/s41398-021-01515-3>

INTRODUCTION

Converging lines of evidence suggest glutamatergic dysfunction is involved in schizophrenia pathophysiology [1–4]. Supporting this view, pharmacological modulation of glutamatergic function via *N*-methyl-D-aspartate receptor (NMDAR) antagonism can induce positive and negative symptoms and cognitive deficits in healthy subjects and exacerbate them in schizophrenia patients [5, 6], with large effect sizes [7]. Genomic studies have identified associations between schizophrenia and variants in genes encoding and/or regulating glutamatergic proteins, including NMDAR and activity-regulated cytoskeleton-associated protein complexes [8–11], which in turn regulate synaptic plasticity and cognition [12–14].

Glutamate levels can be measured in vivo using proton magnetic resonance spectroscopy (¹H-MRS), which indexes total

tissue glutamate, reflecting synaptic glutamate levels, the number of glutamatergic synapses, and extrasynaptic glutamate levels involved in neurometabolism [4, 15]. ¹H-MRS studies have reported elevated glutamate and/or Glx (the sum of glutamate and its metabolite glutamine) levels in patients with schizophrenia in the anterior cingulate cortex (ACC) and medial temporal cortical regions including the hippocampus [16–20], although these data are not unequivocal and may be related to treatment response status.

It has been hypothesised that glutamatergic hyperactivity leads to excitotoxicity-mediated synaptic loss in schizophrenia [3, 21–23]. Supporting this, postmortem studies in schizophrenia have found that cortical glutamatergic neurons display reductions in synaptophysin (a marker of synaptic density), dendritic spine density and

¹MRC London Institute of Medical Sciences, Imperial College London, Hammersmith Hospital Campus, London W12 0NN, UK. ²Institute of Clinical Sciences (ICS), Faculty of Medicine, Imperial College London, London W12 0NN, UK. ³Department of Psychosis Studies, Institute of Psychiatry, Psychology and Neuroscience, King's College London, De Crespigny Park, London SE5 8AF, UK. ⁴South London and Maudsley NHS Foundation Trust, Camberwell, London SE5 8AF, UK. ⁵Department of Brain Sciences, Imperial College London, The Commonwealth Building, Hammersmith Hospital, Du Cane Road, London W12 0NN, UK. ⁶Invicro, Burlington Danes Building, Du Cane Road, London W12 0NN, UK. ⁷Centre for Neuroimaging Sciences, Institute of Psychiatry, Psychology and Neuroscience, King's College London, De Crespigny Park, London SE5 8AF, UK. ⁸Department of Basic and Clinical Neuroscience, Institute of Psychiatry, Psychology and Neuroscience, Maurice Wohl Clinical Neuroscience Institute, King's College London, 5 Cutcombe Road, London SE5 9RT, UK. ⁹MRC Centre for Neurodevelopmental Disorders, King's College London, London SE1 1UL, UK. ✉email: e.onwordi@lms.mrc.ac.uk; oliver.howes@lms.mrc.ac.uk

Received: 21 February 2021 Accepted: 22 June 2021

Published online: 17 July 2021

arborisation [24], and axospinous synaptic density [25] relative to controls. Furthermore, human-derived neurons from schizophrenia patients exhibit deficits in glutamatergic signalling, excitatory postsynaptic currents and synaptic connectivity relative to controls [26–28]. Whilst these findings indicate a link between glutamatergic function and synaptic markers in schizophrenia, it remains unknown if these are related *in vivo* in patients or in the healthy brain.

Synaptic density can now be measured *in vivo* using positron emission tomography (PET) with [¹¹C]UCB-J, a radioligand specific for synaptic vesicle glycoprotein (SV2A), a protein selectively expressed in presynaptic terminals [29]. In a previous study from our laboratory, we found lower SV2A levels in patients relative to controls in the ACC and hippocampus [30], consistent with postmortem evidence for synaptic loss in these regions in schizophrenia [31–33]. If synaptic loss is secondary to ongoing glutamatergic excitotoxicity, SV2A and glutamate levels should be negatively associated. However, the relationship between SV2A and glutamate levels has not been investigated *in vivo*.

Therefore, we conducted a multimodal [¹¹C]UCB-J PET and ¹H-MRS imaging study to test the relationship between the proxy synaptic density marker SV2A and glutamate levels *in vivo*, hypothesising a negative relationship between the two in schizophrenia. Furthermore, levels of the neurometabolite *N*-acetyl aspartate (NAA), which may reflect neuronal integrity [34], are reduced in schizophrenia compared to controls in regions including the ACC and hippocampus [35], potentially secondary to aberrant synaptic elimination [36]. Therefore, we tested the hypothesis that SV2A and NAA levels would be directly associated in schizophrenia. We conducted these tests in the ACC and left hippocampus, given findings for synaptic, glutamatergic and NAA alterations in schizophrenia in these regions [16–19, 30–33, 35].

MATERIALS AND METHODS

The study protocol was approved by the London-West London & GTAC Research Ethics Committee (reference: 16/LO/1941). Approval to administer radioactive material was obtained from the Administration of Radioactive Substances Advisory Committee. All volunteers provided written, informed consent before participating in the study, which was conducted in accordance with the Declaration of Helsinki.

Schizophrenia patient and healthy volunteer recruitment

We recruited 18 patients from mental health services in London and 22 healthy volunteers through public advertisement. Inclusion criteria for all volunteers were: aged between 18 and 65 years old, demonstrated capacity to consent, and had a normal blood coagulation test in advance of arterial blood sampling. Age, gender, ethnicity and smoking status were recorded.

Patients were required to meet DSM-5 criteria for schizophrenia and to have had no changes in treatment for at least 4 weeks prior to the screening visit. Healthy volunteers were required to have no lifetime diagnosis of a mental disorder or family history of psychosis.

Exclusion criteria for all volunteers were: history of neurological disorder, head trauma resulting in a loss of consciousness, drug or alcohol dependence (except for nicotine dependence); significant medical disorder; taking a drug known to interact with SV2A (including levetiracetam, brivaracetam, lorazepam or quinine) [37]; or contraindications to imaging.

Clinical assessments

Schizophrenia patients underwent the Structured Clinical Interview for DSM-5 to confirm the diagnosis and screen for psychiatric co-morbidities. Healthy volunteers were screened with the Structured Clinical Interview for DSM-5 to exclude psychiatric illness, and screened to exclude family history of psychosis.

MR imaging

All subjects underwent structural magnetic resonance imaging (MRI) to facilitate the anatomical delineation of regions of interest (ROIs) and to guide MRS voxel positioning. T1-weighted three-dimension magnetisation-

prepared rapid acquisition gradient echo images were acquired on a Siemens Magnetom Prisma 3T scanner (Siemens, Erlangen, Germany) according to the following parameters: repetition time = 2300.0 ms, echo time = 2.28 ms, flip angle = 9°, field of view = 256 × 256 mm, 176 sagittal slices of 1 mm thickness, voxel size = 1.0 × 1.0 × 1.0 mm.

¹H-MRS acquisition

Single voxel ¹H-MRS was acquired using the Point RESolved technique (TR = 3000 ms, TE = 30 ms, 96 averages, Vector size = 2048, Bandwidth = 2500 Hz). Prior to acquisition of the MRS the B0 homogeneity across the voxel was optimised automatically then fine-tuned manually using the first-order shim gradients to achieve a water linewidth of 18 Hz or less. A voxel measuring 20 × 20 × 20 mm was positioned in the ACC, in the midline immediately anterior to the genu of the corpus callosum (see Supplementary Fig. 1 for voxel placement and example spectrum). A second voxel measuring 20 × 20 × 15 mm was placed in the left hippocampus, angled parallel to the anterior horn of the temporal lobe and positioned just posterior to the amygdala, taking care to avoid the petrous bones (see Supplementary Fig. 2 for voxel placement and example spectrum).

PET imaging

All participants underwent an [¹¹C]UCB-J PET scan as described elsewhere [38]. Briefly, each subject had a CT scan for attenuation correction 2 min prior to radioligand injection. The study physician administered [¹¹C]UCB-J via an intravenous cannula as a smooth bolus injection over 20 s. PET data were acquired for 90 min using a Biograph 6 HiRez PET-CT scanner (Siemens, Erlangen, Germany).

Arterial blood sampling

Radial arterial blood samples were collected throughout the PET scan to measure the arterial input function as described elsewhere [38]. Briefly, whole blood activity was measured using a continuous automatic blood sampling system (Allogg AB, Mariefred, Sweden). Discrete samples were taken at 10, 15, 20, 25, 30, 40, 50, 60, 70, 80 and 90 min after tracer injection. Total radioactivity concentration was evaluated in blood and plasma using a PerkinElmer 1470 10-well gamma counter. Discrete blood samples were used to determine the plasma radioactivity fraction constituted by unchanged parent radioligand using high-performance liquid chromatograph analysis. The [¹¹C]UCB-J plasma free fraction was measured by ultrafiltration in triplicate using an arterial blood sample taken prior to tracer injection.

Image analysis

We used distribution volume ratio (DVR) values as our primary [¹¹C]UCB-J outcome measure for two reasons. First, DVR adjusts for non-specific tracer uptake using a reference region approach. Thus it is thought to reflect more closely the signal specific to SV2A in the region of interest (ROI) than volumes of distribution (V_T) [39], which index both the radioligand concentration specifically bound to SV2A and the nondisplaceable uptake. Second, [¹¹C]UCB-J DVR values show lower variability than V_T values [38] and so likely have greater sensitivity to detect group differences [40], as demonstrated in previous [¹¹C]UCB-J analyses [30]. Notwithstanding this, we conducted exploratory analyses using the volumes of distribution values in addition to the primary analyses using DVR.

Processing and modelling were conducted using MIAKAT version 4.3.7 (<http://www.miakat.org/MIKAT2/index.html>), implemented in MATLAB (Mathworks Inc., Natick, MA, USA) with functions from FSL (version 5.0.10; FMRIB, Oxford, UK) and Statistical and Parametric Mapping12 (SPM12, Wellcome Trust Centre for Neuroimaging, <http://www.fil.ion.ucl.ac.uk/spm>).

Each subject's MRI underwent brain extraction using FSL, and grey matter segmentation and rigid-body coregistration to a standard reference space [41] using SPM12 as implemented via MIAKAT. The template brain image and associated Clinical Imaging Centre atlas [42] were then warped nonlinearly to the individual subject's MRI where the ACC and left hippocampus were defined as ROIs. The centrum semiovale (CS) ROI was generated from the automated anatomical labelling template [43] according to parameters defined for its use as a reference region for nondisplaceable [¹¹C]UCB-J binding [29].

PET images were registered to each subject's MRI and motion-corrected using frame-to-frame rigid-body registration, with the 14th frame (acquired 9–11 min post-injection) as the reference frame. Regional time activity curves (TACs) were generated for each ROI.

Table 1. Clinico-demographic and imaging variables in healthy volunteer (HV) and schizophrenia (SCZ) groups. Values are mean (SEM) or number (*n*).

	HV	SCZ	<i>t</i>	Kolmogorov-Smirnov <i>D</i>	Chi-square	df	<i>p</i>
Age (years)	38.23 [2.59]	40.89 [2.75]	–	0.25	–	–	0.55
Male; Female (<i>n</i>)	21; 1	15; 3	–	–	1.62	–	0.20
Ethnicity							
White; black; other (<i>n</i>)	9; 9; 4	3; 13; 2	–	–	4.03	2	0.13
Current smoker (<i>n</i>)	3	12	–	–	11.88	1	0.0006
Cannabis use within last month (<i>n</i>)	0	2	–	–	2.57	1	0.11
Activity injected	264.40 [5.62]	243.60 [10.88]	–	0.32	–	–	0.25
Plasma free fraction	0.24 [0.005]	0.24 [0.005]	0.82	–	–	38.0	0.42
CS							
[¹¹ C]UCB-J <i>V_T</i>	5.62 [0.12]	5.92 [0.34]	0.91	–	–	38.0	0.37
ACC							
[¹¹ C]UCB-J DVR	3.95 [0.10]	3.48 [0.18]	2.38	–	–	38.0	0.02
[¹¹ C]UCB-J <i>V_T</i>	22.08 [0.67]	19.19 [0.76]	2.87	–	–	38.0	0.007
Glu/Cr	1.10 [0.02]	1.06 [0.02]	1.35	–	–	38.0	0.19
Glx/Cr	1.29 [0.03]	1.31 [0.05]	0.31	–	–	38.0	0.75
NAA/Cr	1.13 [0.02]	1.14 [0.02]	0.04	–	–	38.0	0.97
Left hippocampus							
[¹¹ C]UCB-J DVR	2.67 [0.08]	2.46 [0.14]	1.42	–	–	38.0	0.17
[¹¹ C]UCB-J <i>V_T</i>	14.92 [0.50]	14.17 [0.54]	1.00	–	–	38.0	0.32
Glu/Cr	0.97 [0.03]	0.93 [0.04]	0.78	–	–	37.0	0.44
Glx/Cr	1.38 [0.06]	1.28 [0.07]	1.03	–	–	37.0	0.31
NAA/Cr	1.10 [0.03]	1.07 [0.04]	0.71	–	–	37.0	0.48

Regional TAC and arterial input function data were analysed together using the one-tissue compartment model, which produces reliable estimates of [¹¹C]UCB-J *V_T* [38, 44].

Grey matter masks were applied to the ROIs within MIAKAT to extract regional grey matter *V_T*. Regional DVR was obtained by use of the CS as a pseudoreference region [29, 38].

MRS data were analysed using LC Model[®] 6.3–1L for automatic quantification of in vivo ¹H-MR spectra [45] to index Glu, Glx and NAA concentrations. Glu, Glx and NAA values were scaled to creatine (Cr), which acts as an internal reference. Thus, we report Glu/Cr, Glx/Cr and NAA/Cr levels. Metabolite analyses were restricted to spectra with Cramér-Rao bounds ≤20% and signal-to-noise ratio ≥5%.

Sample size and power calculation

We determined the minimum sample size required to test our primary hypothesis (that there is a negative relationship between synaptic density and glutamate measures). As no previous studies have examined the relationship between SV2A and glutamate measures in the living human brain, we determined that a strong relationship between SV2A and glutamate would be of clinical significance. The power calculation indicated a minimum sample size of 11 per group would have more than 80% power to detect a significant relationship at *r* of 0.7 between these variables, at *p* < 0.05 (two-tailed).

Statistical analysis

Statistical analyses were performed using GraphPad Prism version 6.00 for Mac (GraphPad Software, La Jolla, California, USA (www.graphpad.com)) IBM SPSS Statistics, Version 25, and RStudio Version 1.1.456 (RStudio Team (2016), RStudio, Inc., Boston, MA (<http://www.rstudio.com/>)). We tested data for normality of distribution using the Shapiro–Wilk test. Our primary analysis tested the relationship between grey matter [¹¹C]UCB-J DVR and Glu/Cr and NAA/Cr in the ACC and hippocampus in schizophrenia patients and healthy volunteers using Pearson product-moment correlation, with a Bonferroni-corrected alpha threshold for significance set at 0.0125 for the four tests (0.05/4) in each analysis to control the type I error rate.

For completeness, we also conducted exploratory analyses testing the relationship between grey matter [¹¹C]UCB-J DVR and Glx/Cr, and between grey matter [¹¹C]UCB-J *V_T* and Glu/Cr, Glx/Cr and NAA/Cr, with an uncorrected alpha threshold for significance set at 0.05. Group differences in DVR, *V_T* and neurometabolite levels in the ACC and hippocampus, *V_T* in the CS, and clinico-demographic variables were assessed using two-tailed independent sample *t* tests for normally distributed data, Kolmogorov–Smirnov tests for nonparametric data and Chi-square test for categorical data. Grubbs test was used to identify potential outliers (alpha threshold = 0.05). When demographic variables differed significantly between groups, we tested whether these variables contributed significantly to DVR and neurometabolite levels. When this was the case, we fitted regression models to test whether significant relationships between [¹¹C]UCB-J DVR and neurometabolites survived inclusion of these as covariates.

RESULTS

Forty volunteers (*n* = 18 with schizophrenia [SCZ, 15 male and 3 female] and 22 healthy volunteers [HV, 21 male and 1 female]) completed the study. The groups were well matched in terms of age, gender, ethnicity and recent cannabis use, and there were no significant group differences in mean radioactivity of the PET tracer administered, [¹¹C]UCB-J plasma free fraction or CS [¹¹C]UCB-J *V_T* (Table 1). A significantly greater proportion of the SCZ group were current smokers as compared to the healthy volunteer group (two-tailed Chi-square = 11.88, *p* = 0.0006). Seventeen patients were on antipsychotic medication, and none had co-morbid DSM-5 psychiatric diagnoses. PET data, but not MRS data, from 17 of the patients and 17 healthy volunteers have been used in a separate analysis published recently [30]. The mean (SEM) interval between PET and MRS scans was 53.4 (9.6) days. Spectra quality data are reported in Supplementary Table 1.

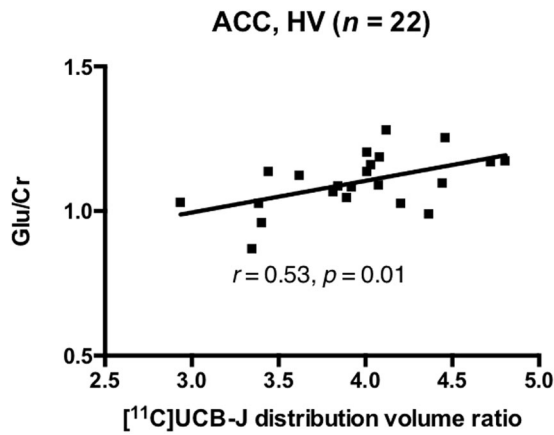


Fig. 1 Synaptic density and glutamate in healthy volunteers. Significant positive relationship between $[^{11}\text{C}]\text{UCB-J}$ distribution volume ratio and Glu/Cr levels in the ACC in the healthy volunteer (HV) group. ACC = anterior cingulate cortex.

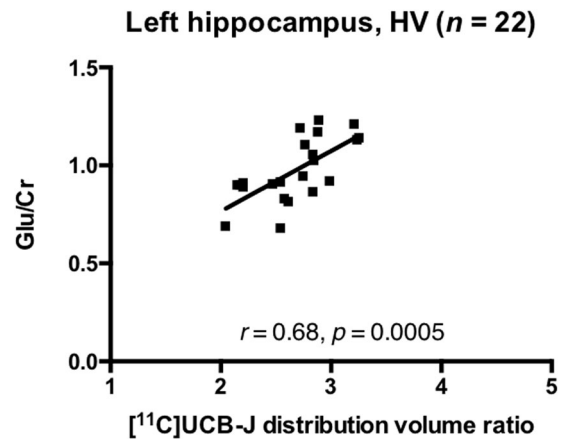


Fig. 3 Synaptic density and glutamate in healthy volunteers. Significant positive relationship between $[^{11}\text{C}]\text{UCB-J}$ distribution volume ratio and Glu/Cr levels in the left hippocampus in the healthy volunteer (HV) group.

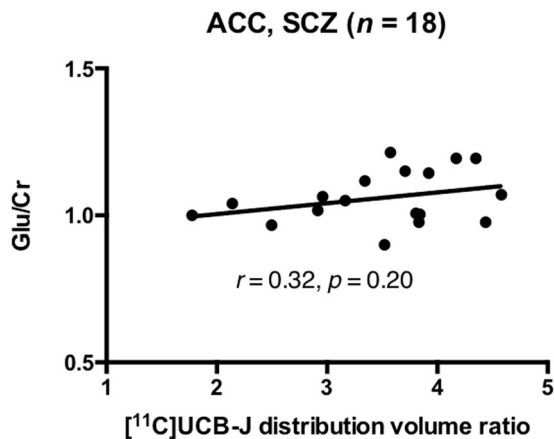


Fig. 2 Synaptic density and glutamate in patients with schizophrenia. No significant relationship between $[^{11}\text{C}]\text{UCB-J}$ distribution volume ratio and Glu/Cr levels in the ACC in the schizophrenia (SCZ) group. ACC = anterior cingulate cortex.

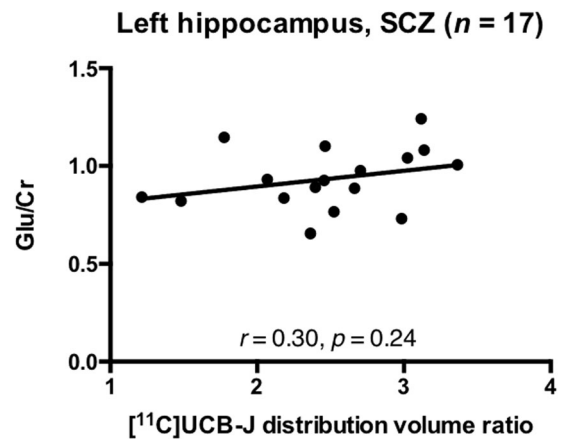


Fig. 4 Synaptic density and glutamate in patients with schizophrenia. No significant relationship between $[^{11}\text{C}]\text{UCB-J}$ distribution volume ratio and Glu/Cr levels in the left hippocampus in the schizophrenia (SCZ) group.

$[^{11}\text{C}]\text{UCB-J}$ DVR and glutamate in the ACC

Mean $[^{11}\text{C}]\text{UCB-J}$ DVR was significantly lower in the SCZ relative to the HV group in the ACC ($t = 2.38$, $p = 0.02$), with a large effect size (Cohen's $d = 0.8$), but there were no significant differences between groups in Glu/Cr or Glx/Cr (Table 1). There was a significant positive relationship between $[^{11}\text{C}]\text{UCB-J}$ DVR and Glu/Cr in the HV ($n = 22$, $r = 0.53$, $p = 0.01$, Fig. 1), but not in the SCZ group ($n = 18$, $r = 0.32$, $p = 0.20$, Fig. 2). Our exploratory analysis found a significant positive relationship between $[^{11}\text{C}]\text{UCB-J}$ DVR and Glx/Cr in the ACC in the HV ($n = 22$, $r = 0.72$, $p = 0.0002$, Supplementary Fig. 3) but not in the SCZ group ($n = 18$, $r = 0.05$, $p = 0.86$, Supplementary Fig. 4).

Post-hoc analysis showed that there was no significant difference between patients and controls in the strength of the bivariate $[^{11}\text{C}]\text{UCB-J}$ DVR-Glu/Cr correlations (Fisher's r -to- $z = 0.74$, $p = 0.46$), but there was a significant difference in the strength of the $[^{11}\text{C}]\text{UCB-J}$ DVR-Glx/Cr correlations ($z = 2.48$, $p = 0.01$).

$[^{11}\text{C}]\text{UCB-J}$ DVR and NAA in the ACC

NAA/Cr levels were not significantly different between groups (Table 1). In the HV group, there was no significant relationship between $[^{11}\text{C}]\text{UCB-J}$ DVR and NAA/Cr in the ACC ($n = 22$, $r = 0.07$,

$p = 0.77$, Supplementary Fig. 5). Although there was a positive relationship between $[^{11}\text{C}]\text{UCB-J}$ DVR and NAA/Cr in the ACC in the SCZ group ($n = 18$, $r = 0.47$, $p = 0.048$, Supplementary Fig. 6), this did not survive Bonferroni correction for multiple comparisons.

$[^{11}\text{C}]\text{UCB-J}$ DVR and glutamate in the left hippocampus

Mean $[^{11}\text{C}]\text{UCB-J}$ DVR was not significantly altered in the SCZ relative to the HV group in the left hippocampus ($t = 1.42$, $p = 0.17$, Cohen's $d = 0.4$). As Cramér-Rao bounds exceeded 20% for one schizophrenia patient's hippocampal Glu/Cr and Glx/Cr data, these data were excluded from the analysis. There were no significant group differences in NAA/Cr, Glu/Cr or Glx/Cr in the left hippocampus (Table 1).

There was a significant positive relationship between $[^{11}\text{C}]\text{UCB-J}$ DVR and Glu/Cr in the hippocampus in the HV group ($n = 22$, $r = 0.68$, $p = 0.0005$, Fig. 3), but not in the SCZ group ($n = 17$, $r = 0.30$, $p = 0.24$, Fig. 4). Our exploratory analysis found a significant relationship between $[^{11}\text{C}]\text{UCB-J}$ DVR and Glx/Cr in the hippocampus in the HV ($n = 22$, $r = 0.48$, $p = 0.03$, Supplementary Fig. 7) but not SCZ group ($n = 17$, $r = 0.16$, $p = 0.53$, Supplementary Fig. 8).

Post-hoc analyses showed that there were no significant differences between patients and controls in the strength of the

bivariate [^{11}C]UCB-J DVR-Glu/Cr (Fisher's r -to- z : $z = 1.46$, $p = 0.14$) or [^{11}C]UCB-J DVR-Glx/Cr ($z = 1.00$, $p = 0.32$) correlations.

[^{11}C]UCB-J DVR and NAA in the hippocampus

There were no significant relationships between [^{11}C]UCB-J DVR and NAA/Cr in the hippocampus in the HV ($n = 22$, $r = 0.23$, $p = 0.31$, Supplementary Fig. 9) or SCZ ($n = 18$, $r = -0.17$, $p = 0.50$, Supplementary Fig. 10) groups.

[^{11}C]UCB-J V_T and neurometabolites

In the ACC, mean [^{11}C]UCB-J V_T was significantly lower in the SCZ relative to the HV group (Table 1), with a large effect size (Cohen's $d = 0.9$). There were no significant relationships between [^{11}C]UCB-J V_T and Glu/Cr, Glx/Cr or NAA/Cr in the ACC in either group (Supplementary Material, Supplementary Figs. 11–16).

In the left hippocampus, mean [^{11}C]UCB-J V_T was not significantly altered in the SCZ relative to the HV group (Cohen's $d = 0.3$, Table 1). There was a significant positive relationship between [^{11}C]UCB-J V_T and Glu/Cr in the hippocampus in the HV but not SCZ group (Supplementary Material, Supplementary Figs. 17–18), although exploratory, post-hoc analyses showed there was no significant difference in the strength of this relationship between groups (Fisher's r -to- z : $z = 1.06$, $p = 0.29$). There were no significant relationships between [^{11}C]UCB-J V_T and Glx/Cr or NAA/Cr (Supplementary Material, Supplementary Figs. 19–22) in either group in the hippocampus.

Effect of smoking status on [^{11}C]UCB-J DVR and neurometabolites

As smoking was more common in the SCZ than HV group, we conducted exploratory analyses to determine if smoking status could influence findings. There was no effect of smoking status on hippocampal Glu/Cr in the SCZ group, on hippocampal [^{11}C]UCB-J DVR, Glx/Cr or NAA/Cr in either group, nor on ACC DVR, Glu/Cr, Glx/Cr or NAA/Cr in either group (see Supplementary Material). However, in the HV group, hippocampal Glu/Cr was significantly lower in smokers (smokers = 0.88 [0.03]; non-smokers = 0.99 [0.04]; $t = 2.28$, $df = 13.2$, $p = 0.04$). Nevertheless, the significant relationship between [^{11}C]UCB-J DVR and Glu/Cr in the left hippocampus in the HV group remained after including smoking status in a regression model ($r = 0.69$, $p = 0.002$).

DISCUSSION

Our main finding is that [^{11}C]UCB-J DVR is positively correlated with glutamate levels in the ACC and hippocampus in healthy volunteers, but not in patients with schizophrenia. [^{11}C]UCB-J indexes SV2A, a presynaptic protein ubiquitously expressed in nerve terminals, and SV2A levels are closely related to other synaptic density markers such as synaptophysin [29, 46]. Thus, our findings extend *ex vivo* evidence that a large proportion of mammalian hippocampal and neocortical synapses are glutamatergic [47–53], by providing *in vivo* evidence for this in healthy humans as well. Moreover, our findings suggest synaptic density and glutamate levels are not related to the same degree in schizophrenia.

Our finding that [^{11}C]UCB-J binding is significantly lower in the ACC in patients relative to controls is consistent with previous findings [30] in a cohort that largely overlaps with the sample in this study. In contrast, left hippocampal [^{11}C]UCB-J V_T and DVR values were not significantly different between groups, although they were lower in schizophrenia in absolute terms. Our previous finding of significantly lower [^{11}C]UCB-J DVR in the hippocampus in schizophrenia compared to healthy volunteers related to both hippocampi [30], whereas our findings here relate only to the left hippocampus. Moreover, compared to the ACC, hippocampal [^{11}C]UCB-J V_T values show a lower signal-to-noise ratio with 42–90% greater variance in healthy hippocampal V_T values relative to total V_T [30, 54]. Thus, the lack of a significant group difference in left hippocampal [^{11}C]UCB-J

binding may reflect a lack of power. We did not find significant group differences in Glu/Cr, Glx/Cr and NAA/Cr, in contrast to findings from systematic reviews and meta-analyses [16, 18, 55, 56] but consistent with previous individual case-control studies of a similar size [57–61]. This likely reflects a lack of power to detect group differences of modest effect size as observed in meta-analysis. Importantly, it should be recognised that our study was not designed to detect group differences in these measures, but the relationship between [^{11}C]UCB-J and the MRS measures.

Strengths and limitations

We deployed multimodal imaging to investigate for the first time *in vivo* the relationship between a synaptic terminal marker and neurometabolites in the human brain. [^{11}C]UCB-J shows good test–retest reproducibility, indicating it is a reliable imaging tool [44]. All but one of the schizophrenia subjects were taking antipsychotic medication. Recent studies found no effect of haloperidol or olanzapine administration on SV2A protein levels or specific binding in the rat brain, suggesting antipsychotic treatment is unlikely to affect the [^{11}C]UCB-J measure in schizophrenia patients [30, 62]. There is some, albeit inconsistent evidence that antipsychotic drug administration may reduce glutamate levels in schizophrenia, with four of eight of published studies showing significant reductions (in the frontal and left temporal cortices, left thalamus and right striatum) following antipsychotic drug administration in schizophrenia while the other half show no significant change [63]. Notwithstanding this inconsistency, given that most of our patients were taking antipsychotics, it would be valuable to confirm our findings in unmedicated patients. There were significantly more smokers in the schizophrenia group than in the healthy volunteer group in our study. Furthermore, in the healthy volunteer group, we found that Glu/Cr levels were significantly lower in smokers. Previous studies have shown that smokers display lower cortical glutamate levels than non-smokers [64, 65]. Thus, our results may be confounded by differences in smoking levels across groups. However, we found that Glu/Cr levels did not differ significantly between groups and that smoking status did not alter the significant relationship between [^{11}C]UCB-J DVR and Glu/Cr in the healthy volunteer group. Nonetheless, future studies should seek to control for smoking status between groups, and additionally to explore the relationship between quantity of smoking and glutamate levels. A potential limitation is that two subjects with schizophrenia had cannabis use within the last month, although this is a small and nonsignificant difference compared to healthy volunteers, and we excluded substance dependence in all volunteers through clinical assessment. Therefore, cannabis use is unlikely to have a marked effect on our findings. Nonetheless, it would be valuable to repeat these tests in a sample of patients entirely free of cannabis use. As our study does not probe GABA concentrations, we are unable to evaluate the relative densities of excitatory and inhibitory synapses in the healthy brain or in schizophrenia. In addition, at 3T, glutamate and glutamine are challenging to quantify due to considerable spectral overlap [66, 67]. Higher field strengths are needed to more precisely separate glutamate and glutamine signals. Creatine was used as an internal reference, which could affect analyses if there are creatine alterations in schizophrenia [68]. However, meta-analyses of brain creatine levels in schizophrenia have not found significant alterations, indicating this is unlikely to be a major factor in our analyses [55, 69]. As this was a cross-sectional study, it is not possible to delineate the precise mechanistic relationship between glutamate and SV2A *in vivo*. Animal models and patient-derived neuronal lines are needed to test the underlying mechanisms to establish directions of causality.

The primary outcome measure was DVR, estimated using the centrum semiovale as a reference region, given the evidence for very low specific binding levels in that region [29, 70]. The

centrum semiovale is a white matter region largely devoid of SV2A and with very low [^{11}C]UCB-J uptake [29, 38, 44, 70]. Nonetheless it displays a small amount of displacement of [^{11}C]UCB-J uptake by levetiracetam, a drug selective for SV2A [29], suggesting some specific binding. Blocking studies have shown this is approximately 8% of that in grey matter, causing a slight underestimation of specific binding in grey matter, and white matter may not be an optimal reference region given its distinct tissue composition compared to grey matter [39]. Therefore, a group difference in centrum semiovale specific binding could bias our results. However, we did not find a significant difference between groups in centrum semiovale V_T , consistent with our previous results [30]. This suggests differences in centrum semiovale specific binding are not driving our findings, and supports its suitability as a reference region in [^{11}C]UCB-J PET in schizophrenia.

Although we found a significant difference between patients and controls in the strength of the [^{11}C]UCB-J DVR-Glx/Cr correlations in the ACC, we found no such differences between groups in the hippocampus, nor between groups in the strength of the [^{11}C]UCB-J DVR-Glu/Cr correlations in either region of interest, nor between groups in the strength of the [^{11}C]UCB-J V_T -Glu/Cr correlation in the hippocampus, using Fisher's r -to- z transformation test. It should be noted that this study was not designed to test differences in the relative strengths of correlations, and is likely underpowered for these purposes, which would require a substantially greater difference in correlation strengths or a substantially larger study, or both.

Implications for understanding the ^1H -MRS glutamate signal

Our findings have implications for understanding the origin of the glutamate signal as captured by ^1H -MRS. The highest brain glutamate concentrations are found in glutamatergic nerve terminals, with glial and extracellular glutamate levels kept low [71, 72]. Moreover, previous studies have reported that glutamate immunostaining intensity is significantly positively correlated with synaptic vesicle density ($r = 0.94$ in hippocampal mossy fibre terminals and $r = 0.27$ in Golgi cell terminals) [73] and that metabolic and neurotransmitter glutamate pools are tightly correlated [74]. These findings, taken with ours of a significant relationship between SV2A and glutamate in the ACC and hippocampus in the healthy brain, support the hypothesis that glutamate levels measured by ^1H -MRS reflect the concentration of glutamate in the presynaptic neurotransmitter pool in the ACC and hippocampus [75–77]. It should also be noted that our findings are in keeping with preliminary *in vivo* evidence in a mixed sample of healthy volunteers and patients with Alzheimer's disease showing a significant positive association between SV2A binding and metabotropic glutamate subtype 5 receptors (mGluR5) binding via radioligand [^{18}F]FPEB, a potential marker of glutamatergic neurotransmission, and a significant mGluR5-by-region of interest interaction effect on [^{11}C]UCB-J V_T [78]. Interestingly, in Mecca's work, there was no effect of diagnosis on the relationship between mGluR5 and SV2A binding [78].

Implications for understanding the ^1H -MRS NAA signal

[^{11}C]UCB-J binding was not related to NAA levels in either group in the ACC or hippocampus. NAA concentrations have been interpreted as potentially reflecting synaptic levels [36, 79–82]. However, our findings indicate NAA levels are not closely related to synaptic density in adulthood. NAA is synthesised in mitochondria and localised to synaptic terminals, dendritic arborisations, neuronal somata and fine axons [83]. Its levels may be affected by the broad range of processes in which it is involved, including myelin lipid synthesis, mitochondrial energy production, and synthesis of *N*-acetylaspartylglutamate [34]. Taken with the above, our findings that little of the variance in NAA levels measured *in vivo* is related to synaptic terminal levels in

healthy volunteers or schizophrenia, indicate caution should be exercised before using NAA as proxy for synaptic terminal levels and/or synaptic elimination, and may suggest neurometabolism contributes more to its variance. Further work is warranted, however, to explore whether synaptic loss in the ACC is associated with lower levels of NAA measured by ^1H -MRS in schizophrenia and other neuropsychiatric disorders.

Implications for understanding schizophrenia

Our finding that [^{11}C]UCB-J binding and glutamate levels are not related in either ROI in patients does not support our hypothesis that ongoing glutamatergic hyperactivity underlies synaptic alterations in schizophrenia. However, the lower synaptic density marker levels, taken with the loss of the normal relationship between this and glutamate levels in the ACC, could be explained by a loss of glutamatergic terminals in schizophrenia, such that a greater proportion of the remaining SV2A protein signal is from GABAergic synapses. This possibility is supported by postmortem [24, 25, 84] and other findings indicating excitatory-inhibitory imbalance in schizophrenia [85–88]. Another possibility is that a greater proportion of the glutamate signal is extra-synaptic, and thus unrelated to SV2A, in schizophrenia. Supporting this, there is evidence potentially for altered regulation of glutamate reuptake into synapses in schizophrenia [24, 71, 89]. These putative deficits are not mutually exclusive, and further work is needed to establish which is the main determinant of our findings. Notwithstanding this, our findings extend preclinical and clinical evidence for frontal cortical and hippocampal dysfunction in schizophrenia [90–95], to suggest this includes an altered relationship between synaptic terminal and glutamate levels.

CONCLUSIONS

Levels of [^{11}C]UCB-J binding, a synaptic terminal marker, are significantly positively correlated with Glu/Cr levels in the ACC and hippocampus in healthy volunteers, but not in schizophrenia. These findings indicate that an appreciable proportion of the ^1H -MRS glutamatergic signal is related to synaptic density in healthy volunteers. They are not consistent with our hypothesis that current glutamatergic excitotoxicity leads to synaptic loss in schizophrenia, but do indicate the normal relationship between glutamate and synaptic terminal levels is disrupted, potentially due to lower levels of glutamatergic synapses and/or a reduced proportion of glutamatergic synapses in the anterior cingulate cortex in schizophrenia.

DATA AVAILABILITY

Imaging and related clinical data will be made available upon reasonable request.

CODE AVAILABILITY

Code used to generate findings reported in this article will be made available upon reasonable request.

REFERENCES

- Howes O, McCutcheon R, Stone J. Glutamate and dopamine in schizophrenia: an update for the 21st century. *J Psychopharmacol*. 2015;29:97–115.
- Moghaddam B, Javitt D. From revolution to evolution: the glutamate hypothesis of schizophrenia and its implication for treatment. *Neuropsychopharmacology*. 2012;37:4–15.
- Goff DC, Coyle JT. The emerging role of glutamate in the pathophysiology and treatment of schizophrenia. *Am J Psychiatry*. 2001;158:1367–77.
- McCutcheon RA, Krystal JH, Howes OD. Dopamine and glutamate in schizophrenia: biology, symptoms and treatment. *World Psychiatry*. 2020;19:15–33.
- Javitt DC, Zukin SR. Recent advances in the phencyclidine model of schizophrenia. *Am J Psychiatry*. 1991;148:1301–8.
- Krystal JH, Karper LP, Seibyl JP, Freeman GK, Delaney R, Bremner JD, et al. Sub-anesthetic effects of the noncompetitive NMDA antagonist, ketamine, in humans.

- Psychotomimetic, perceptual, cognitive, and neuroendocrine responses. *Arch Gen Psychiatry*. 1994;51:199–214.
7. Beck K, Hindley G, Borgan F, Ginestet C, McCutcheon R, Brugger S, et al. Association of ketamine with psychiatric symptoms and implications for its therapeutic use and for understanding schizophrenia: a systematic review and meta-analysis. *JAMA Netw Open*. 2020;3:e204693.
 8. Fromer M, Pocklington AJ, Kavanagh DH, Williams HJ, Dwyer S, Gormley P, et al. De novo mutations in schizophrenia implicate synaptic networks. *Nature*. 2014;506:179–84.
 9. Purcell SM, Moran JL, Fromer M, Ruderfer D, Solovieff N, Roussos P, et al. A polygenic burden of rare disruptive mutations in schizophrenia. *Nature*. 2014;506:185–90.
 10. Kirov G, Pocklington AJ, Holmans P, Ivanov D, Ikeda M, Ruderfer D, et al. De novo CNV analysis implicates specific abnormalities of postsynaptic signalling complexes in the pathogenesis of schizophrenia. *Mol Psychiatry*. 2012;17:142–53.
 11. Cross-Disorder Group of the Psychiatric Genomics Consortium Electronic address: @. Cross-Disorder Group of the Psychiatric Genomics C. Genomic relationships, novel loci, and pleiotropic mechanisms across eight psychiatric disorders. *Cell*. 2019;179:1469–82.e1411.
 12. Malenka RC, Nicoll RA. NMDA-receptor-dependent synaptic plasticity: multiple forms and mechanisms. *Trends Neurosci*. 1993;16:521–7.
 13. Shepherd JD, Bear MF. New views of Arc, a master regulator of synaptic plasticity. *Nat. Neurosci*. 2011;14:279–84.
 14. Bramham CR, Alme MN, Bittins M, Kuipers SD, Nair RR, Pai B, et al. The Arc of synaptic memory. *Exp. Brain Res*. 2010;200:125–40.
 15. Poels EM, Kegeles LS, Kantrowitz JT, Javitt DC, Lieberman JA, Abi-Dargham A, et al. Glutamatergic abnormalities in schizophrenia: a review of proton MRS findings. *Schizophr. Res*. 2014;152:325–32.
 16. Mouchlianitis E, McCutcheon R, Howes OD. Brain-imaging studies of treatment-resistant schizophrenia: a systematic review. *Lancet Psychiatry*. 2016;3:451–63.
 17. Kraguljac NV, White DM, Reid MA, Lahti AC. Increased hippocampal glutamate and volumetric deficits in unmedicated patients with schizophrenia. *JAMA Psychiatry*. 2013;70:1294–302.
 18. Merritt K, Egerton A, Kempton MJ, Taylor MJ, McGuire PK. Nature of glutamate alterations in schizophrenia: a meta-analysis of proton magnetic resonance spectroscopy studies. *JAMA Psychiatry*. 2016;73:665–74.
 19. van Elst LT, Valerius G, Büchert M, Thiel T, Rüschi N, Bubl E, et al. Increased prefrontal and hippocampal glutamate concentration in schizophrenia: evidence from a magnetic resonance spectroscopy study. *Biol Psychiatry*. 2005;58:724–30.
 20. Demjaha A, Egerton A, Murray RM, Kapur S, Howes OD, Stone JM, et al. Antipsychotic treatment resistance in schizophrenia associated with elevated glutamate levels but normal dopamine function. *Biol Psychiatry*. 2014;75:e11–3.
 21. Olney JW, Farber NB. Glutamate receptor dysfunction and schizophrenia. *Arch Gen Psychiatry*. 1995;52:998–1007.
 22. Olney JW, Labruyere J, Price MT. Pathological changes induced in cerebrotal neurons by phencyclidine and related drugs. *Science*. 1989;244:1360–2.
 23. Glantz LA, Gilmore JH, Lieberman JA, Jarskog LF. Apoptotic mechanisms and the synaptic pathology of schizophrenia. *Schizophr Res*. 2006;81:47–63.
 24. Hu W, MacDonald ML, Elswick DE, Sweet RA. The glutamate hypothesis of schizophrenia: evidence from human brain tissue studies. *Ann NY Acad Sci*. 2015;1338:38–57.
 25. Roberts RC, et al. Ultrastructural evidence for glutamatergic dysregulation in schizophrenia. *Schizophr Res*. 2020. <https://www.sciencedirect.com/science/article/abs/pii/S0920996420300323?via%3Dihub>.
 26. Brennand KJ, Simone A, Joo J, Gelboin-Burkhardt C, Tran N, Sangar S, et al. Modelling schizophrenia using human induced pluripotent stem cells. *Nature*. 2011;473:221–5.
 27. Wen Z, Nguyen HN, Guo Z, Lalli MA, Wang X, Su Y, et al. Synaptic dysregulation in a human iPSC cell model of mental disorders. *Nature*. 2014;515:414–8.
 28. Yu DX, Di Giorgio FP, Yao J, Marchetto MC, Brennand K, Wright R, et al. Modeling hippocampal neurogenesis using human pluripotent stem cells. *Stem Cell Rep*. 2014;2:295–310.
 29. Finnema SJ, Nabulsi NB, Eid T, Detynecki K, Lin SF, Chen MK, et al. Imaging synaptic density in the living human brain. *Sci Transl Med*. 2016;8:348ra96.
 30. Onwordi EC, et al. Synaptic density marker SV2A is reduced in schizophrenia patients and unaffected by antipsychotics in rats. *Nat Commun*. 2020;11.
 31. Feinberg I. Schizophrenia: caused by a fault in programmed synaptic elimination during adolescence? *J Psychiatr Res*. 1982;17:319–34.
 32. Keshavan MS, Anderson S, Pettegrew JW. Is Schizophrenia due to excessive synaptic pruning in the prefrontal cortex? The Feinberg hypothesis revisited. *J Psychiatr Res*. 1994;28:239–65.
 33. Osimo EF, Beck K, Reis Marques T, Howes OD. Synaptic loss in schizophrenia: a meta-analysis and systematic review of synaptic protein and mRNA measures. *Mol Psychiatry*. 2019;24:549–61.
 34. Moffett JR, Ross B, Arun P, Madhavarao CN, Nambodiri AM. N-Acetylaspartate in the CNS: from neurodiagnostics to neurobiology. *Prog. Neurobiol*. 2007;81:89–131.
 35. Whitehurst TS, Osugo M, Townsend L, Shatalina E, Vava R, Onwordi EC, et al. Proton magnetic resonance spectroscopy of n-acetyl aspartate in chronic schizophrenia, first episode of psychosis and high-risk of psychosis: a systematic review and meta-analysis. *Neurosci. Biobehav Rev*. 2020;119:255–67.
 36. Boksa P. Abnormal synaptic pruning in schizophrenia: urban myth or reality? *J. Psychiatry Neurosci*. 2012;37:75–7.
 37. Danish A, Namasivayam V, Schiedel AC, Muller CE. Interaction of approved drugs with synaptic vesicle protein 2A. *Arch. Pharm*. 2017;350:3–4.
 38. Mansur A, et al. Characterization of 3 PET Tracers for Quantification of Mitochondrial and Synaptic Function in Healthy Human Brain: (18)F-BCPP-EF,(11)C-SA-4503, and (11)C-UCB-J. *J Nucl Med*. 2020;61:96–103.
 39. Rossano S, et al. Assessment of a white matter reference region for (11)C-UCB-J PET quantification. *J Cereb Blood Flow Metab*. 2019;271678X19879230.
 40. Bloomfield PS, Selvaraj S, Veronese M, Rizzo G, Bertoldo A, Owen DR, et al. Microglial activity in people at ultra high risk of psychosis and in schizophrenia: an [(11)C]PBR28 PET brain imaging study. *Am. J. Psychiatry*. 2016;173:44–52.
 41. Larsen R, Nielsen M, Sparring J (eds). Symmetric atlas and model based segmentation: an application to the hippocampus in older adults. *medical image computing and computer-assisted intervention—MICCAI 2006*. Berlin, Heidelberg: Springer Berlin Heidelberg; 2006.
 42. Tziortzi AC, Searle GE, Tzimopoulou S, Salinas C, Beaver JD, Jenkinson M, et al. Imaging dopamine receptors in humans with [11C](+)-PHNO: dissection of D3 signal and anatomy. *Neuroimage*. 2011;54:264–77.
 43. Tzourio-Mazoyer N, Landeau B, Papathanassiou D, Crivello F, Etard O, Delcroix N, et al. Automated anatomical labeling of activations in SPM using a macroscopic anatomical parcellation of the MNI MRI single-subject brain. *NeuroImage*. 2002;15:273–89.
 44. Finnema SJ, Nabulsi NB, Mercier J, Lin SF, Chen MK, Matuskey D, et al. Kinetic evaluation and test-retest reproducibility of [(11)C]UCB-J, a novel radioligand for positron emission tomography imaging of synaptic vesicle glycoprotein 2A in humans. *J Cereb Blood Flow Metab*. 2018;38:2041–52.
 45. Provencher SW. Automatic quantitation of localized in vivo 1H spectra with LCModel. *NMR Biomed*. 2001;14:260–4.
 46. Bajjalieh SM, Frantz GD, Weimann JM, McConnell SK, Scheller RH. Differential expression of synaptic vesicle protein 2 (SV2) isoforms. *J. Neurosci*. 1994;14:5223–35.
 47. Beaulieu C, Colonnier M. A laminar analysis of the number of round-asymmetrical and flat-symmetrical synapses on spines, dendritic trunks, and cell bodies in area 17 of the cat. *J Comp Neurol*. 1985;231:180–9.
 48. Beaulieu C, Kisvarday Z, Somogyi P, Cynader M, Cowey A. Quantitative distribution of GABA-immunopositive and-immunonegative neurons and synapses in the monkey striate cortex (Area 17). *Cereb Cortex*. 1992;2:295–309.
 49. Somogyi P, Tamas G, Lujan R, Buhl EH. Salient features of synaptic organisation in the cerebral cortex. *Brain Res Brain Res Rev*. 1998;26:113–35.
 50. Mel BW, Schiller J. On the fight between excitation and inhibition: location is everything. *Sci STKE*. 2004;2004:PE44.
 51. Megias M, Emri Z, Freund TF, Gulyas AI. Total number and distribution of inhibitory and excitatory synapses on hippocampal CA1 pyramidal cells. *Neuroscience*. 2001;102:527–40.
 52. Liu G. Local structural balance and functional interaction of excitatory and inhibitory synapses in hippocampal dendrites. *Nat Neurosci*. 2004;7:373–9.
 53. Sahara S, Yanagawa Y, O'Leary DD, Stevens CF. The fraction of cortical GABAergic neurons is constant from near the start of cortical neurogenesis to adulthood. *J Neurosci*. 2012;32:4755–61.
 54. Holmes SE, Scheinost D, Finnema SJ, Naganawa M, Davis MT, DellaGioia N, et al. Lower synaptic density is associated with depression severity and network alterations. *Nat Commun*. 2019;10:1529.
 55. Kraguljac NV, Reid M, White D, Jones R, den Hollander J, Lowman D, et al. Neurometabolites in schizophrenia and bipolar disorder - a systematic review and meta-analysis. *Psychiatry Res*. 2012;203:111–25.
 56. Steen RG, Hamer RM, Lieberman JA. Measurement of brain metabolites by 1H magnetic resonance spectroscopy in patients with schizophrenia: a systematic review and meta-analysis. *Neuropsychopharmacology*. 2005;30:1949–62.
 57. Hutcherson NL, Reid MA, White DM, Kraguljac NV, Avsar KB, Bolding MS, et al. Multimodal analysis of the hippocampus in schizophrenia using proton magnetic resonance spectroscopy and functional magnetic resonance imaging. *Schizophr Res*. 2012;140:136–42.
 58. Théberge J, Bartha R, Drost DJ, Menon RS, Malla A, Takhar J, et al. Glutamate and glutamine measured with 4.0 T proton MRS in never-treated patients with schizophrenia and healthy volunteers. *Am J Psychiatry*. 2002;159:1944–6.
 59. Kraguljac NV, Reid MA, White DM, den Hollander J, Lahti AC. Regional decoupling of N-acetyl-aspartate and glutamate in schizophrenia. *Neuropsychopharmacology*. 2012;37:2635–42.

60. Borgan FR, Jauhar S, McCutcheon RA, Pepper FS, Rogdaki M, Lythgoe DJ, et al. Glutamate levels in the anterior cingulate cortex in un-medicated first episode psychosis: a proton magnetic resonance spectroscopy study. *Sci Rep.* 2019;9:8685.
61. Korenic SA, Klingaman EA, Wickwire EM, Gaston FE, Chen H, Wijtenburg SA, et al. Sleep quality is related to brain glutamate and symptom severity in schizophrenia. *J Psychiatr Res.* 2020;120:14–20.
62. Halff EF, Cotel MC, Natesan S, McQuade R, Ottley CJ, Srivastava DP, et al. Effects of chronic exposure to haloperidol, olanzapine or lithium on SV2A and NLGN synaptic puncta in the rat frontal cortex. *Behav Brain Res.* 2021;405:113203.
63. Egerton A, Bhachu A, Merritt K, McQueen G, Szulc A, McGuire P. Effects of anti-psychotic administration on brain glutamate in schizophrenia: a systematic review of longitudinal (1)H-MRS studies. *Front Psychiatry.* 2017;8:66.
64. Faulkner P, et al. Daily and intermittent smoking are associated with low prefrontal volume and low concentrations of prefrontal glutamate, creatine, myoinositol, and N-acetylaspartate. *Addict Biol* 2020: e12986.
65. Durazzo TC, Meyerhoff DJ, Mon A, Abé C, Gazdzinski S, Murray DE. Chronic cigarette smoking in healthy middle-aged individuals is associated with decreased regional brain N-acetylaspartate and glutamate levels. *Biol Psychiatry.* 2016;79:481–8.
66. Pradhan S, Bonekamp S, Gillen JS, Rowland LM, Wijtenburg SA, Edden RA, et al. Comparison of single voxel brain MRS AT 3T and 7T using 32-channel head coils. *Magn Reson Imaging.* 2015;33:1013–8.
67. Snyder J, Wilman A. Field strength dependence of PRESS timings for simultaneous detection of glutamate and glutamine from 1.5 to 7T. *J Magn Reson.* 2010;203:66–72.
68. Ongur D, Prescott AP, Jensen JE, Cohen BM, Renshaw PF. Creatine abnormalities in schizophrenia and bipolar disorder. *Psychiatry Res.* 2009;172:44–8.
69. Iwata Y, Nakajima S, Plitman E, Mihashi Y, Caravaggio F, Chung JK, et al. Neuro-metabolite levels in antipsychotic-naïve/free patients with schizophrenia: a systematic review and meta-analysis of 1 H-MRS studies. *Prog Neuro-Psychopharmacol Biol Psychiatry.* 2018;86:340–52.
70. Varnas K, Stepanov V, Hallidin C. Autoradiographic mapping of synaptic vesicle glycoprotein 2A in non-human primate and human brain. *Synapse.* 2020;74: e22157.
71. Danbolt NC. Glutamate uptake. *Prog Neurobiol.* 2001;65:1–105.
72. Bramham CR, Torp R, Zhang N, Storm-Mathisen J, Ottersen OP. Distribution of glutamate-like immunoreactivity in excitatory hippocampal pathways: a semi-quantitative electron microscopic study in rats. *Neuroscience.* 1990;39:405–17.
73. Ji ZQ, Aas JE, Laake J, Walberg F, Ottersen OP. An electron-microscopic, immunogold analysis of glutamate and glutamine in terminals of rat spinocerebellar fibers. *J Comp Neurol.* 1991;307:296–310.
74. Sibson NR, Dhankhar A, Mason GF, Rothman DL, Behar KL, Shulman RG. Stoichiometric coupling of brain glucose metabolism and glutamatergic neuronal activity. *Proc Natl Acad Sci USA.* 1998;95:316–21.
75. Gallinat J, Kunz D, Senkowski D, Kienast T, Seifert F, Schubert F, et al. Hippocampal glutamate concentration predicts cerebral theta oscillations during cognitive processing. *Psychopharmacology.* 2006;187:103–11.
76. Yuksel C, Ongur D. Magnetic resonance spectroscopy studies of glutamate-related abnormalities in mood disorders. *Biol Psychiatry.* 2010;68:785–94.
77. Horder J, Petrinovic MM, Mendez MA, Bruns A, Takumi T, Sporeen W, et al. Glutamate and GABA in autism spectrum disorder—a translational magnetic resonance spectroscopy study in man and rodent models. *Transl Psychiatry.* 2018;8:106.
78. Mecca AP, Chen MK, Godek TA, Harris JE, Bartlett HH, Toyonaga T, et al. P2-349: association between Mglur5 and synaptic density: a multi-tracer study of healthy aging and Alzheimer's disease. *Alzheimer's Dement.* 2019;15:P729.
79. Yeo RA, Hill D, Campbell R, Vigil J, Brooks WM. Developmental instability and working memory ability in children: a magnetic resonance spectroscopy investigation. *Dev. Neuropsychol.* 2000;17:143–59.
80. Glantz LA, Lewis DA. Decreased dendritic spine density on prefrontal cortical pyramidal neurons in schizophrenia. *Arch. Gen. Psychiatry.* 2000;57:65–73.
81. Demougeot C, Marie C, Giroud M, Beley A. N-acetylaspartate: a literature review of animal research on brain ischaemia. *J. Neurochem.* 2004;90:776–83.
82. Roberts RC, Barksdale KA, Roche JK, Lahti AC. Decreased synaptic and mitochondrial density in the postmortem anterior cingulate cortex in schizophrenia. *Schizophr. Res.* 2015;168:543–53.
83. Moffett JR, Nambodiri MA, Neale JH. Enhanced carbodiimide fixation for immunohistochemistry: application to the comparative distributions of N-acetylaspartylglutamate and N-acetylaspartate immunoreactivities in rat brain. *J. Histochem Cytochem.* 1993;41:559–70.
84. Glausier JR, Lewis DA. Dendritic spine pathology in schizophrenia. *Neuroscience.* 2013;251:90–107.
85. McCutcheon RA, Reis Marques T, Howes OD. Schizophrenia—an overview. *JAMA Psychiatry.* 2019:1–10.
86. Krystal JH, Anticevic A, Yang GJ, Dragoi G, Driesen NR, Wang XJ, et al. Impaired tuning of neural ensembles and the pathophysiology of schizophrenia: a translational and computational neuroscience perspective. *Biol. Psychiatry.* 2017;81:874–85.
87. Kehrer C, Maziashvili N, Dugladze T, Gloveli T. Altered excitatory-inhibitory balance in the NMDA-hypofunction model of schizophrenia. *Front Mol Neurosci.* 2008;1:6.
88. Insel TR. Rethinking schizophrenia. *Nature.* 2010;468:187–93.
89. Pillinger T, Rogdaki M, McCutcheon RA, Hathway P, Egerton A, Howes OD. Altered glutamatergic response and functional connectivity in treatment resistant schizophrenia: the effect of riluzole and therapeutic implications. *Psychopharmacology.* 2019;236:1985–97.
90. Adams RA, et al. Impaired theta phase coupling underlies frontotemporal dysconnectivity in schizophrenia. *Brain.* 2020;143:1261–77.
91. Lieberman JA, Girgis RR, Brucato G, Moore H, Provenzano F, Kegeles L, et al. Hippocampal dysfunction in the pathophysiology of schizophrenia: a selective review and hypothesis for early detection and intervention. *Mol Psychiatry.* 2018;23:1764–72.
92. Lodge DJ, Grace AA. Hippocampal dysregulation of dopamine system function and the pathophysiology of schizophrenia. *Trends Pharm Sci.* 2011;32:507–13.
93. Heckers S. Neuroimaging studies of the hippocampus in schizophrenia. *Hippocampus.* 2001;11:520–8.
94. Tamminga CA, Stan AD, Wagner AD. The hippocampal formation in schizophrenia. *Am J Psychiatry.* 2010;167:1178–93.
95. Brugger SP, Howes OD. Heterogeneity and homogeneity of regional brain structure in schizophrenia: a meta-analysis. *JAMA Psychiatry.* 2017;74:1104–11.

ACKNOWLEDGEMENTS

The authors thank the patients and healthy volunteers who participated in this study, and Rohini Akosa, Ryan Janisch, Daniela Ribeiro, Jim Anscombe and Dr. Maja Ranger for their expert assistance. ODH acknowledges financial support for this study from the Medical Research Council (grant nos. MC-A656–5QD30 and MR/L022176/1), Wellcome Trust (no. 094849/Z/10/Z) and the National Institute for Health Research (NIHR) Biomedical Research Centre at South London and Maudsley NHS Foundation Trust and King's College London.

AUTHOR CONTRIBUTIONS

Conceptualisation: ECO. and ODH. Data curation: ECO. Formal analysis: ECO and ODH. Funding acquisition: TRM. and ODH. Investigation: ECO., TW, BS, AB, MQ and MR. Methodology: ECO, AM, and ODH. Project administration: ECO, SN and ODH. Resources: BS, DOR, and ODH. Software: AM. Supervision: ACV and ODH. Validation: AM, EAR and RNG. Visualisation: ECO. Writing—original draft: ECO. Writing—review and editing: all authors.

COMPETING INTERESTS

AM, EAR and RNG are employees of Invivo LLC. RNG is a consultant for AbbVie, Biogen & Cerveau. TRM has received honoraria for speaking and chairing from Lundbeck, Janssen and Astellas, and received honoraria to participate in advisory boards organised by Angelini Pharmaceuticals. ODH is a part-time employee of H Lundbeck A/v and has received investigator-initiated research funding from and/or participated in advisory/speaker meetings organised by Angelini, Astra-Zeneca, Autifony, Biogen, BMS, Eli Lilly, Heptares, Janssen, Lundbeck, Lyden-Delta, Otsuka, Servier, Sunovion, Rand and Roche. Neither ODH nor his family have holdings/a financial stake in any pharmaceutical company. The other authors declare no competing interests. The opinions expressed in this study are solely those of the authors and should not be taken as representing those of the NIHR, NHS, Lundbeck or any other organisation.

ADDITIONAL INFORMATION

Supplementary information The online version contains supplementary material available at <https://doi.org/10.1038/s41398-021-01515-3>.

Correspondence and requests for materials should be addressed to E.C.O. or O.D.H.

Reprints and permission information is available at <http://www.nature.com/reprints>

Publisher's note Springer Nature remains neutral with regard to jurisdictional claims in published maps and institutional affiliations.

Ethical standards: The authors assert that all procedures contributing to this work comply with the ethical standards of the relevant national and institutional committees on human experimentation and with the Helsinki Declaration of 1975, as revised in 2008.



Open Access This article is licensed under a Creative Commons Attribution 4.0 International License, which permits use, sharing, adaptation, distribution and reproduction in any medium or format, as long as you give appropriate credit to the original author(s) and the source, provide a link to the Creative Commons license, and indicate if changes were made. The images or other third party material in this article are included in the article's Creative Commons license, unless indicated otherwise in a credit line to the material. If material is not included in the article's Creative Commons license and your intended use is not permitted by statutory regulation or exceeds the permitted use, you will need to obtain permission directly from the copyright holder. To view a copy of this license, visit <http://creativecommons.org/licenses/by/4.0/>.

© The Author(s) 2021